Dicle University
Journal of Engineering

https://dergipark.org.tr/tr/pub/**dumf**
duje.dicle.edu.tr

Electronic Behavior and Optical Properties of New Ferromagnetic Silver-Based Sulfo-spinel: AgV_2S_4

Buğra YILDIZ[1*], Aytaç ERKİŞİ[2]

[1] Hacettepe University, Physics Engineering Department, bugrayildiz@hacettepe.edu.tr, Orcid No: 0000-0002-0080-7096

[2] Pamukkale University, Department of Physics, aerkisi@pau.edu.tr, Orcid No: 0000-0001-7995-7590

ARTICLE INFO	ABSTRACT

This study reports the intriguing properties of a novel ternary silver-based sulfo-spinel vanadium system (AgV_2S_4) having a face centered cubic structure (FCC). The magnetic nature, electronic behavior and optical properties of this system are revealed. The calculations were performed with spin-effect and by using generalized gradient approximation (GGA) under Density Functional Theory (DFT). After obtaining the optimized Wyckoff positions for the atoms in the crystal structure of this composition, it was decided that this spinel material has ferromagnetic nature in view of the energy-volume curves obtained for three different magnetic phases and of the calculated cohesive energies. Furthermore, the spin-polarized electronic band structure with the orbital projected density of electronic states was calculated within the first principles to investigate its behavior and bonding characteristic in detail. The observed small band gap in the minority spin channel is $E_g = 0.41$ eV, so its electronic band structure implies that this system has half-metallic character. Finally, to evaluate some optical features, frequency-dependent complex dielectric functions were calculated. Then, some optical properties were investigated by using the real and imaginary parts of the dielectric function.

Introduction

Chalco-spinels, has face centered cubic structure with 14 atoms in primitive cell and conform 227 space number with $Fd\overline{3}m$ space group and the base are usually chosen from transition metals [1-3]. They have attracted a lot of attention since they have been practiced in several applications thanks to their semiconductor or half-metallic behavior and due to their high absorbency [4, 5]. So far, they have been used in many varieties of applications such as; magneto- and electro-optics, biomedical, spin-based electronic devices, data storage applications and magnetic refrigeration applications [6-10]. Although, there are many theoretical and experimental studies about this type of chalco-spinels, many of them still waiting for to be discovered [11-18]. Among them, chromium chalco-spinels are one of the most studied compounds. It has intriguing electronic and magnetic features such as magnetic resistivity [19], semiconducting nature [20, 21] and magnetocapacitance [22, 23].

Another widely studied compounds in this family due to its electronic and optical properties are AB_2S_4 types ternary sulfo-spinels. Especially, refrigerant ability and magnetic capacitance of $CdCr_2S_4$ is one of the main focuses of experimental studies [24-26]. Even though similar materials have studied extensively, the electronic, magnetic and optical feature of AgV_2S_4 is not broadly researched, as far as we know from the literature. For the mentioned reason, this study is very important and could shed light on future theoretical and experimental studies.

This study presents the ferromagnetic nature, half-metallicity and optical aspects of silver-based vanadium sulfo-spinel (AgV_2S_4) system discovered by *DFT* calculations by using the VASP package. In the presented computational study, the magnetic nature of this spinel system has been understood to be ferromagnetic and then spin-dependent electronic band structure has been investigated to collect information about its electronic behavior in ferromagnetic order. Also, some optical properties of this silver-based sulfo-spinel system has been investigated and complex dielectric function, refractive index, extinction coefficient, absorption coefficient, and loss function have been computed. The material could be a good candidate for photovoltaic applications due to its high absorbency and the spin-down band gap in its electronic band structure.

Computational details

In order to understand electronic, magnetic and optical properties of this sulfo-spinel system, VASP (Vienna Ab-initio Simulation Package) [27-28] has been employed under the DFT (Density Functional Theory). Throughout the process, Kohn-Sham equations [29] were solved iteratively until all the forces and pressures on each atom become zero and PBE (Perdew-Burke-Ernzerhof) type correlation functionals were considered within the GGA (Generalized Gradient Approximations) [30]. Also, the PAW (projector-augmented) method [31] has been used to describe interactions between the ion cores and electrons. Valance electron configurations are $5s^14d^{10}$, $3p^63d^44s^1$ and $3s^23p^4$ for Ag, V and S atoms respectively.

In addition, $10\times10\times10$ MP (Monkhorst and Pack) scheme k-point mesh has been used and it has created 110 k-points in the Brillouin zone [32]. The cut off energy has been selected as 700 eV. Methfessel–Paxton type smearing method has been considered and 0.01 eV smearing parameter has been chosen. Relaxation processes continued until the minimum force on each atom reach 10^{-8} eV/Å and 10^{-9} eV iteration steps has been employed. Furthermore, optical properties of the sulfo-spinel vanadium system (AgV_2S_4) have been investigated with the calculated complex dielectric function.

Results and discussion

In this theoretical work, firstly, the primitive cell of the silver-based vanadium sulfo-spinel AgV_2S_4 was properly optimized by placing the ions in the most appropriate Wyckoff positions of the cell. Thus, optimized structural parameters were achieved with high accuracy. The primitive lattice of this system consists of 14 atoms and it has face centered cubic structure with 227 space number and conforms $Fd\bar{3}m$ space group. For the optimized crystal, the Wyckoff positions of two silver (Ag) atoms, four vanadium (V) atoms and eight sulphur (S) atoms were 16d (0.5, 0.5, 0.5), 8a (0.125, 0.125, 0.125) and 32e (0.362, 0.362, 0.362) respectively. Also, three-dimensional crystallographic shape of the mentioned material is presented in Figure 1.
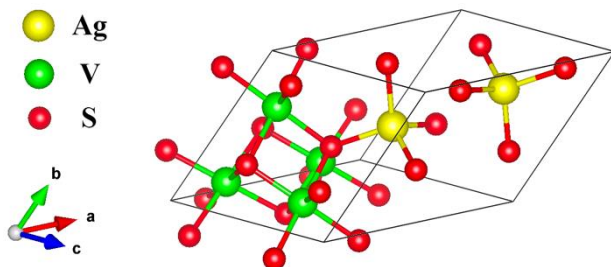

Figure 1. Three-dimensional crystal structure of AgV_2S_4 compound. The yellow, green, and red spheres represent silver (Ag), vanadium (V), and sulphur (S) atoms respectively.

The structural properties

To determine the ground state magnetic structure, antiferromagnetic (AFM), ferromagnetic (FM) and paramagnetic (PM) types of magnetic phases have been considered. For the antiferromagnetic phase, the magnetic moments of the vanadium (V) atoms were aligned antiparallel and they yield zero-net magnetization and for the ferromagnetic phase magnetic moments of the atoms are oriented in the same direction. Finally for the paramagnetic phase all the magnetic moments are zero. After that, cohesive energies have been calculated for each magnetic arrangement. The cohesive energy is defined as the energy required to disengage the crystal into free atoms and it could be determined by using the total energy difference between the bulk crystal and isolated free atoms [33] as the equation given below:

$$E_{Coh} = E_{AgV_2S_4} - (2E_{Ag}^{iso} + 4E_V^{iso} + 8E_S^{iso}) \qquad (1)$$

where, E_{Ag}^{iso}, E_V^{iso} and E_S^{iso} are the isolated ground state energies for silver (Ag), vanadium (V) and sulphur (S) atoms, respectively, while $E_{AgV_2S_4}$ is the total ground state energy of the primitive cell. According to this definition, the structures with larger negative cohesive energy are more favorable energetically, while the system with positive energy cannot be spontaneously emerged in nature. The calculated cohesive energy values, the lattice parameters and atomic bond lengths are tabulated in Table 1 for this system under consideration. For each magnetic phase considered, the calculated cohesive energies imply that the FM phase is more stable energetically since the value of the cohesive energy of this phase is less than PM and AFM phase. In this respect, the negative value of the calculated cohesive energy indicates that this vanadium sulfo-spinel is thermodynamically stable [34] so it could be synthesized and can be used in some technological applications. The plotted energy-volume graph, which is obtained by using the Vinet equation of states [35], is shown in Figure 2. The energy-volume plot shows that the ground state phases of this system are ferromagnetic with approximately 0.09 eV lower energy than AFM phase for AgV_2S_4. For the compound, PM phase has higher energies than both FM and AFM phases indicating an unfavorable crystal structure energetically. This result is compatible with the cohesive energy results which are shown at Table 1.

Table 1. The optimized primitive cell lattice parameter (a) and atomic bond lengths (d) for the stable ferromagnetic phase and the calculated cohesive energies (E_{coh}) of silver-based vanadium sulfo-spinel (AgV$_2$S$_4$) for ferromagnetic, antiferromagnetic and paramagnetic phases.

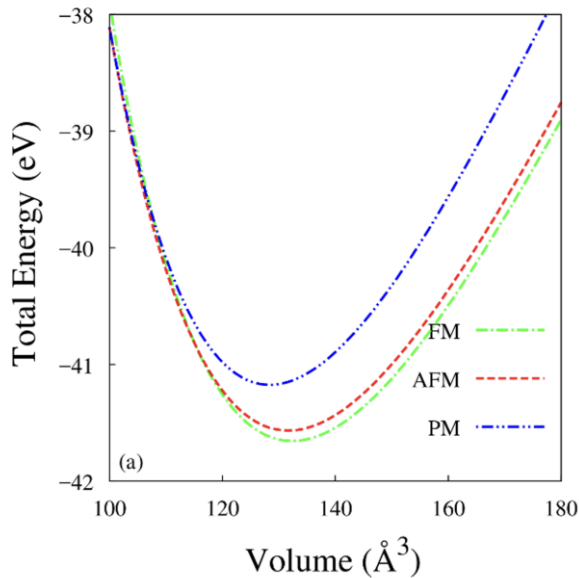| *Material*	*a* (Å)	$d_{Ag\text{-}S}$ (Å)	$d_{V\text{-}S}$ (Å)	E_{Coh} (eV)
AgV$_2$S$_4$	7.206 (FM)	2.444 (FM)	2.419 (FM)	-20.119 (FM)
				-20.030 (AFM)
				-19.637 (PM)

Figure 2. Total energies versus volumes of the primitive cell in ferromagnetic, antiferromagnetic and paramagnetic orders of AgV$_2$S$_4$.

As seen in Table 2, considering the computed partial magnetic moments, the predominance of vanadium (*V*) atoms is clearly noticeable, since the compound has ferromagnetic nature. Also, the fact that the total magnetic moment of this material is relatively large which highlights its ferromagnetic character.

Table 2. The calculated total magnetic moment (μ_{tot}) of the ferromagnetic silver-based sulfo-spinel compound (AgV$_2$S$_4$) and the partial magnetic moments (μ_{atom}) of Ag, V and S atoms in this system.

Material	$\mu_{tot}(\mu_B)$	$\mu_{atom}(\mu_B)$
AgV$_2$S$_4$	5.735	μ_{Ag} = -0.065
		μ_V = 1.687
		μ_S = -0.111

The Curie temperature (T_c) is another important parameter to understand behavior of magnetic moments. At this critical temperature, the arrangement of magnetic moments changes drastically, in other words, the magnetic nature of the compound undergoes a phase transition. Curie temperature is especially crucial for ferromagnetic systems and it could be determined from the ground state energies of FM and AFM phases by using mean field approximation [36-39] (MFA) as follows:

$$\frac{3}{2}k_B T_c^{MFA} = E_{AFM} - E_{FM} \qquad (2)$$

where k_B is the Boltzman constant. The computed ground state energies for the antiferromagnetic and ferromagnetic phases of this sulfo-spinel and the predicted Curie temperature according to the mean field approximation are given in Table 3.

Table 3. The computed ground state energies for the paramagnetic and ferromagnetic phases for AgV$_2$S$_4$ and estimated Curie temperature (T_c in *K*).

Material	E_{AFM} (eV)	E_{FM} (eV)	T_c^{MFA} (K)
AgV$_2$S$_4$	-20.784	-20.829	348

The electronic properties

In order to find out electronic behavior, after ferromagnetic character has been understood, electronic band structure with total (TDOS) and partial density of states (PDOS) were examined under spin effect. The density of states is determined within generalized gradient approximation (GGA) and it is constructed for spin-up and spin-down channels along high-symmetry directions in the Brillouin zone in Figure 3. As clearly seen from the plotted figure, this sulfo-spinel system could be classified as half-metallic material due to having a small band gap (E$_g$ = 0.41 eV) in its spin-down channel, while its spin-up channel behaves

like metallic. The observed band gap is a direct one at Γ-point. Moreover, the fact that the band structure drawn for spin up and down channels differ from each other demonstrates that the compound is not paramagnetic. Also, this result is consistent with the previous result.

In order to understand the atomic projection of this half-metallic material [40], the total (TDOS) and the orbital projected partial density of electronic states of atoms (PDOS) are plotted as seen in Figure 4. In the figure, it could be seen that, the hybridizations between the *d* states of silver (*Ag*) and vanadium (*V*) atoms and the *3p* states of the sulphur (*S*) around the Fermi energy level (E_F). For AgV$_2$S$_4$ system, below and near the Fermi level (E_F), the *3d* states of vanadium (*V*) atoms (almost between 0 and -0.5 eV energy range) are dominant and in the valance band the *3p* states of the sulphur (*S*) atoms are more effective between 0 and -4 eV. The above the Fermi level is known as conducting band where the *d* orbitals of the vanadium (*V*) atoms are dominant. The same dominancy of this state of vanadium (*V*) atoms stands out around 1.7 eV. Also, there are hybridizations between *d* orbitals of vanadium (*V*) atoms and *p* orbitals of sulphur (*S*) atoms between 0 and 0.7 eV and between 2.7 eV and 3.7 eV.

It could be seen that around the Fermi level, the main contribution comes from the *d* orbitals of the vanadium (*V*) atoms and the *p* orbital of the sulphur (*S*) atom. So that the half-metallic character of this spinel system can mainly be attributed to *d*-orbitals of vanadium (*V*) atoms and *p*-orbitals of sulphur (*S*) atoms. As a result, it could be concluded that the *s* orbitals of atoms in this material and *p* orbitals of silver (*Ag*) and vanadium (*V*) atoms don't have much effect on the formation and chemical bonding.

The complex dielectric function and optical characteristics

The complex dielectric function, which is among the optical properties of any solid crystal, calculated as a function of frequency with its real (ε^{real}) and imaginary (ε^{img}) parts. It can provide important information about electronic polarizability and electric charge storage capability. Also, this complex function given by Eq. 3 can determine the optical response of a solid material at all photon energies.

$$\varepsilon(\omega) = \varepsilon^{real}(\omega) + i\varepsilon^{img}(\omega) \qquad (3)$$

The imaginary part of the related function describes the ability to absorb light and can be calculated by using the dipole matrix and Fermi distribution for the occupied states in the valence band and the unoccupied states in the conduction band [41, 42] whereas the real part computed from the Kramers-Kronig transformation, is related the electronic polarizability. The equations required to calculate the imaginary part of this function are given in Ref. [43, 44]. In this part of this study, as given in Figures 5a and 5b, the electronic and ionic contributions to the frequency-dependent dielectric function of the material have been computed separately ($\varepsilon(\omega) = \varepsilon_{elec}(\omega) + \varepsilon_{ion}(\omega)$). The electronic contribution [45] to the real and

imaginary parts of the dielectric constant can be calculated with the help of the equation above while the ionic contribution [46] to the dielectric constant can be calculated by density functional perturbation theory (DFPT). As shown in Figure 5a, the real and imaginary parts of the electronic contributions (ε_e^{real} and ε_e^{img}) to the dielectric function were plotted in the 0-8 eV photon energy range while the ionic contributions (ε_i^{real} and ε_i^{img}) to the dielectric function were plotted in the 0-68 eV range.

In the plots, it was observed that the real parts of electronic contribution have negativity indicating metallic behavior in the 0.63 - 1.25 eV and 3.77 - 8 eV energy ranges for AgV$_2$S$_4$. The material shows metallic character when the external electric field at frequencies higher than plasma frequency is applied.

Furthermore, some important optical parameters such as refractive index $(n(\omega))$, extinction coefficient $(\kappa(\omega))$, absorption coefficient $(I(\omega))$ and loss function $(L(\omega))$ were computed from given equations in below [47] and plotted in Fig.6;

$$n(\omega) = \sqrt{\frac{\sqrt{\varepsilon_r^2(\omega) + \varepsilon_i^2(\omega)} + \varepsilon_r(\omega)}{2}} \qquad (4)$$

$$\kappa(\omega) = \sqrt{\frac{\sqrt{\varepsilon_r^2(\omega) + \varepsilon_i^2(\omega)} - \varepsilon_r(\omega)}{2}} \qquad (5)$$

$$I(\omega) = \omega \sqrt{2\sqrt{\varepsilon_r^2(\omega) + \varepsilon_i^2(\omega)} - 2\varepsilon_r(\omega)} \qquad (6)$$

$$L(\omega) = \frac{\varepsilon_i(\omega)}{\varepsilon_r^2(\omega) + \varepsilon_i^2(\omega)} \qquad (7)$$

As seen in Figure 6, the static refractive index values ($n(0)$) have been calculated for the case where the frequency is equal to zero within the GGA approximation. For the low energy region refractive index ($n(\omega)$) starts from 3.2 and shows a sudden trend of increase.

The observed maximum peaks are 6.2 around 0.31 eV energy (mid-infrared region) for AgV$_2$S$_4$. In addition, it was observed that the frequency-dependent refractive index values obtained for the high energy region tended to decrease. The value of the extinction coefficient, which is another important optical parameter, calculated depending on the frequency, shows a sharp peak of 5.4 at 0.34 eV.

The absorption capability of the incident photon which has a specific frequency can be determined from the computed absorption coefficient *I(ω)*. Moreover, this interesting parameter points out whether any material which has a suitable band gap and high absorption coefficient *I(ω)* can be used in photovoltaic applications [48]. This compound could be a good candidate for photovoltaic applications due to its high absorbency and the minority band gap in its electronic band structure. Finally, among optical properties,

the loss function gives significant information about the energy loss of fast electrons traversing the compound. The observed maximums in the mentioned spectrums can be related with as plasmon oscillations [49].
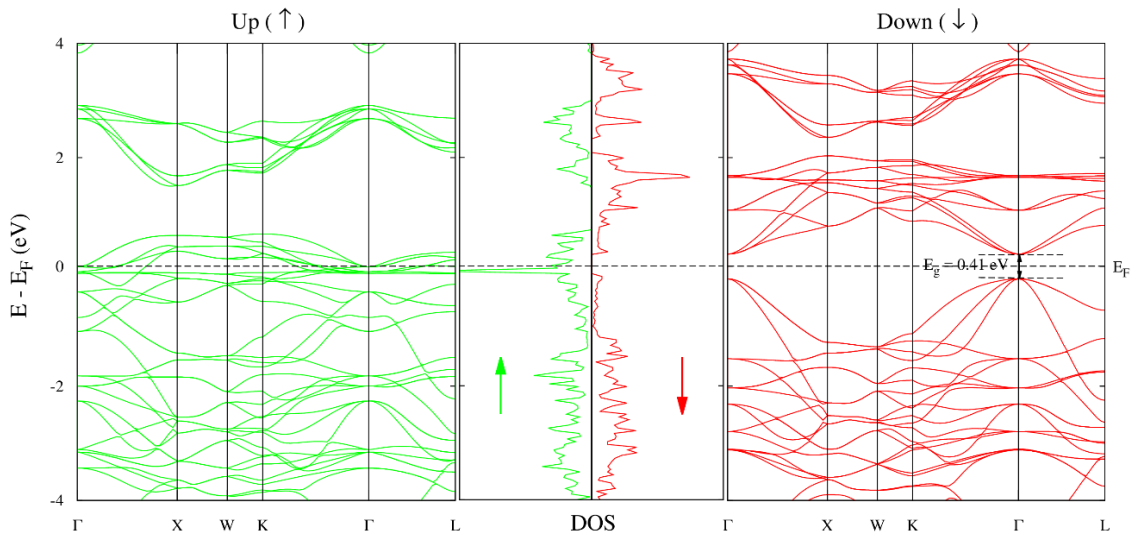

Figure 3. The calculated spin-polarized energy band structure with the total density of electronic states within generalized gradient approximation of sulfo-spinel AgV$_2$S$_4$.
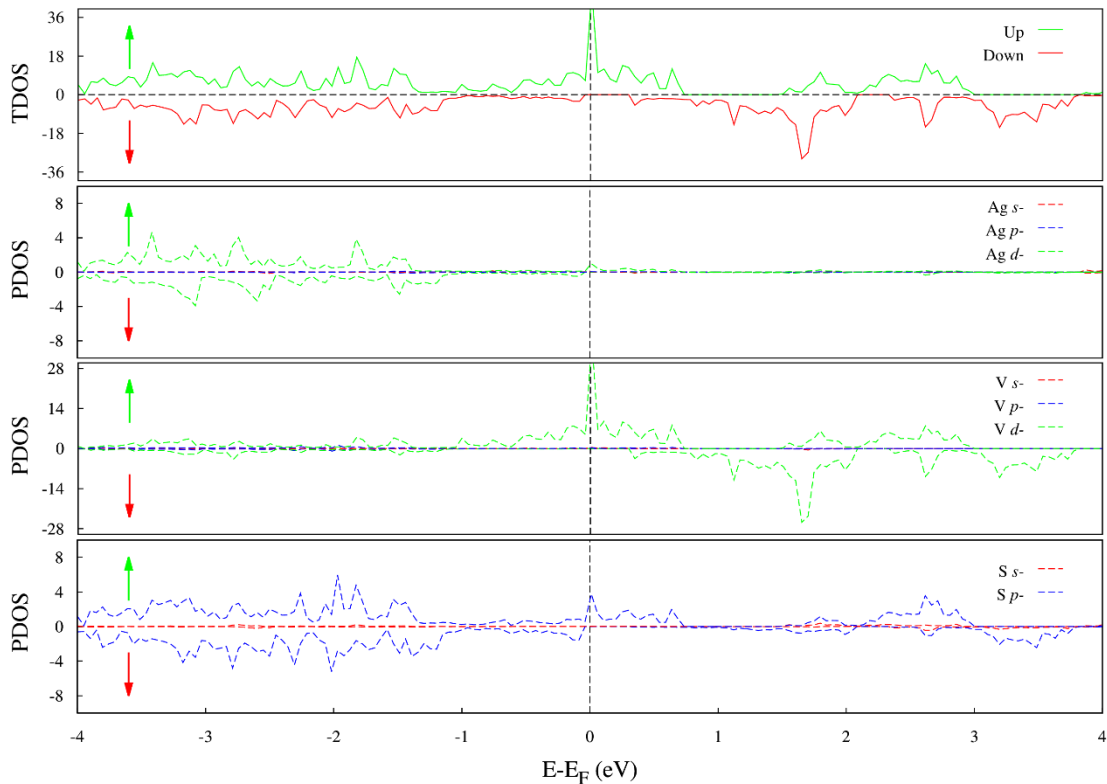

Figure 4. The total (TDOS) and orbital projected partial density of electronic states of atoms (PDOS) within GGA of sulfo-spinel AgV$_2$S$_4$.
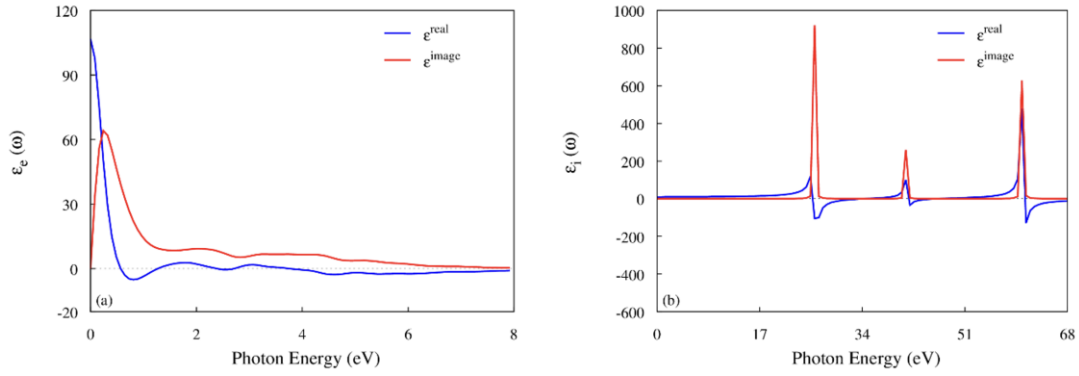
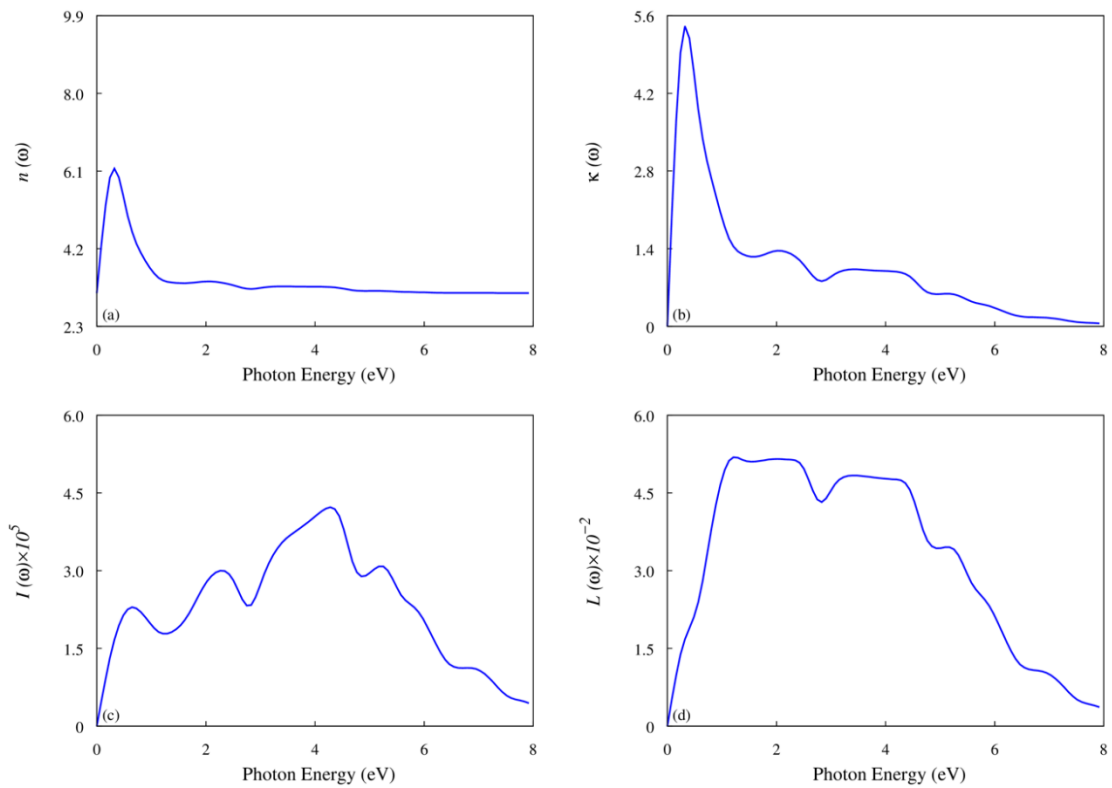Figure 5. (a) The electronic contribution and (b) ionic contribution to the complex dielectric function of AgV$_2$S$_4$.

Figure 6. Spectra of (a) refractive index $(n(\omega))$, (b) extinction coefficient $(\kappa(\omega))$, (c) absorption coefficient $(I(\omega))$ and

(d) loss function $(L(\omega))$ of AgV$_2$S$_4$ sulfo-spinel.

Conclusion

In this theoretical research, in order to reveal the electronic behavior, magnetic nature and optical properties, comprehensive *DFT* calculations have been performed for ternary silver-based vanadium (AgV$_2$S$_4$) sulfo-spinel. It has been optimized in face centered cubic structure which conforms 227 space number with $Fd\bar{3}m$ space group. The most stable phase for this material is ferromagnetic phase since it has ground state energy. This result is also confirmed by the calculated cohesive energies. Considering the calculated electronic band structure, the electronic character of this sulfo-spinel system is half-metallic due to a narrow band gap of E$_g$ = 0.41 eV in its spin-down channel, while spin-up channel exhibit metallic behavior. With this half-metallic property, the material can be a good candidate for spintronic applications. Furthermore, the investigated optical properties show that the mentioned sulfo-spinel can promise to be used in photovoltaic applications due to their high absorbency and the spin-down band gap in its electronic band structure.

Ethics committee approval and conflict of interest statement

"There is no need to obtain permission from the ethics committee for the article prepared"

"There is no conflict of interest with any person / institution in the article prepared"

Authors' Contributions

-Study conception and design: Yıldız, Erkişi

-Acquisition of data: Erkişi

-Analysis and interpretation of data: Yıldız

-Drafting of manuscript: Yıldız, Erkişi

-Critical revision: Yıldız, Erkişi

Acknowledgement

References

[1]   I. Efthimiopoulos *et al.*, "Structural transition in the magnetoelectric spinel under pressure," *Phys. Rev. B*, vol. 93, no. 17, p. 174103, May 2016, doi: 10.1103/PhysRevB.93.174103.

[2]   C. J. Fennie and K. M. Rabe, "Polar phonons and intrinsic dielectric response of the ferromagnetic insulating spinel CdCr2S4 *Phys. Rev. B*, vol. 72, no. 21, p. 214123, Dec. 2005, doi: 10.1103/PhysRevB.72.214123.

[3]   H. Sims, K. Ramasamy, W. H. Butler, and A. Gupta, "Electronic structure of magnetic semiconductor CdCr 2 Te 4 : A possible spin-dependent symmetry filter," *Appl. Phys. Lett.*, vol. 103, no. 19, p. 192402, Nov. 2013, doi: 10.1063/1.4827818.

[4]   A. Erkişi, "Ab Initio Study on Electronic and Elastic Properties of AgCr 2 S 4," *Acta Phys. Pol. A*, vol. 140, no. 3, pp. 243–251, Sep. 2021, doi: 10.12693/APhysPolA.140.243.

[5]   A. Erkisi, B. Yildiz, X. Wang, M. Isik, Y. Ozcan, and G. Surucu, "The investigation of electronic nature and mechanical properties under spin effects for new half-metallic ferromagnetic chalcogenides Ag3CrX4 (X = S, Se, and Te)," *J. Magn. Magn. Mater.*, vol. 519, p. 167482, Feb. 2021, doi: 10.1016/j.jmmm.2020.167482.

[6]   R. F. Ziolo *et al.*, "Matrix-Mediated Synthesis of Nanocrystalline γ-Fe 2 O 3 : A New Optically Transparent Magnetic Material," *Science (80-.).*, vol. 257, no. 5067, pp. 219–223, Jul. 1992, doi: 10.1126/science.257.5067.219.

[7]   S. Sun, C. B. Murray, D. Weller, L. Folks, and A. Moser, "Monodisperse FePt Nanoparticles and Ferromagnetic FePt Nanocrystal Superlattices," *Science (80-.).*, vol. 287, no. 5460, pp. 1989–1992, Mar. 2000, doi: 10.1126/science.287.5460.1989.

[8]   D. Yoo, H. Jeong, S.-H. Noh, J.-H. Lee, and J. Cheon, "Magnetically Triggered Dual Functional Nanoparticles for Resistance-Free Apoptotic Hyperthermia," *Angew. Chemie Int. Ed.*, vol. 52, no. 49, pp. 13047–13051, Dec. 2013, doi: 10.1002/anie.201306557.

[9]   H. Zeng, J. Li, J. P. Liu, Z. L. Wang, and S. Sun, "Exchange-coupled nanocomposite magnets by nanoparticle self-assembly," *Nature*, vol. 420, no. 6914, pp. 395–398, Nov. 2002, doi: 10.1038/nature01208.

[10]   R. Hao, R. Xing, Z. Xu, Y. Hou, S. Gao, and S. Sun, "Synthesis, Functionalization, and Biomedical Applications of Multifunctional Magnetic Nanoparticles," *Adv. Mater.*, vol. 22, no. 25, pp. 2729–2742, Jul. 2010, doi: 10.1002/adma.201000260.

[11]   A. S. Cameron *et al.*, "Magnetic phase diagram of the helimagnetic spinel compound ZnCr 2 Se 4 revisited by small-angle neutron scattering," *J. Phys. Condens. Matter*, vol. 28, no. 14, p. 146001, Apr. 2016, doi: 10.1088/0953-8984/28/14/146001.

[12]   N. Menyuk, K. Dwight, R. J. Arnott, and A. Wold, "Ferromagnetism in CdCr 2 Se 4 and CdCr 2 S 4," *J. Appl. Phys.*, vol. 37, no. 3, pp. 1387–1388, Mar. 1966, doi: 10.1063/1.1708484.

[13]   M. Tachibana, N. Taira, and H. Kawaji, "Heat capacity and thermal expansion of CdCr2Se4 and CdCr2S4," *Solid State Commun.*, vol. 151, no. 23, pp. 1776–1779, Dec. 2011, doi: 10.1016/j.ssc.2011.08.029.

[14]   S. Kitani, M. Tachibana, and H. Kawaji, "Spin-glass-like behavior in ferromagnetic phase of CdCr2S4," *Solid State Commun.*, vol. 179, pp. 16–19, Feb. 2014, doi: 10.1016/j.ssc.2013.06.004.

[15]   K. Ramasamy, D. Mazumdar, R. D. Bennett, and A. Gupta, "Syntheses and magnetic properties of

Cr2Te3 and CuCr2Te4 nanocrystals," *Chem. Commun.*, vol. 48, no. 45, p. 5656, 2012, doi: 10.1039/c2cc32021e.

[16] T. Kanomata, H. Ido, and T. Kaneko, "Effect of Pressure on Curie Temperature of Calcogenide Spinels CuCr 2 X 4 (X=S, Se and Te)," *J. Phys. Soc. Japan*, vol. 29, no. 2, pp. 332–335, Aug. 1970, doi: 10.1143/JPSJ.29.332.

[17] T. Suzuyama *et al.*, "Ferromagnetic-phase transition in the spinel-type CuCr2Te4," *J. Solid State Chem.*, vol. 179, no. 1, pp. 140–144, Jan. 2006, doi: 10.1016/j.jssc.2005.10.007.

[18] R. Li, C. Zhang, and Y. Zhang, "Critical properties of the 3D-Heisenberg ferromagnet CuCr2Te4," *Solid State Commun.*, vol. 152, no. 3, pp. 173–176, Feb. 2012, doi: 10.1016/j.ssc.2011.11.014.

[19] H. W. Lehmann and M. Robbins, "Electrical Transport Properties of the Insulating Ferromagnetic Spinels CdCr 2 S 4 and CdCr 2 Se 4," *J. Appl. Phys.*, vol. 37, no. 3, pp. 1389–1390, Mar. 1966, doi: 10.1063/1.1708485.

[20] P. K. Baltzer, H. W. Lehmann, and M. Robbins, "Insulating Ferromagnetic Spinels," *Phys. Rev. Lett.*, vol. 15, no. 11, pp. 493–495, Sep. 1965, doi: 10.1103/PhysRevLett.15.493.

[21] K. G. Nikiforov, "Magnetically ordered multinary semiconductors," *Prog. Cryst. Growth Charact. Mater.*, vol. 39, no. 1–4, pp. 1–104, Jan. 1999, doi: 10.1016/S0960-8974(99)00016-9.

[22] J. Hemberger, P. Lunkenheimer, R. Fichtl, H.-A. Krug von Nidda, V. Tsurkan, and A. Loidl, "Relaxor ferroelectricity and colossal magnetocapacitive coupling in ferromagnetic CdCr2S4," *Nature*, vol. 434, no. 7031, pp. 364–367, Mar. 2005, doi: 10.1038/nature03348.

[23] S. Weber, P. Lunkenheimer, R. Fichtl, J. Hemberger, V. Tsurkan, and A. Loidl, "Colossal Magnetocapacitance and Colossal Magnetoresistance in HgCr$_2$S$_4$," *Phys. Rev. Lett.*, vol. 96, no. 15, p. 157202, Apr. 2006, doi: 10.1103/PhysRevLett.96.157202.

[24] V. Tsurkan, D. Ehlers, V. Felea, H.-A. Krug von Nidda, and A. Loidl, "Critical magnetic behavior of ferromagnetic CdCr$_2$S$_4$," *Phys. Rev. B*, vol. 88, no. 14, p. 144417, Oct. 2013, doi: 10.1103/PhysRevB.88.144417.

[25] L. Q. Yan *et al.*, "Large magnetocaloric effect in spinel CdCr2S4," *Appl. Phys. Lett.*, vol. 90, no. 26, p. 262502, Jun. 2007, doi: 10.1063/1.2751576.

[26] C. P. Sun *et al.*, "Colossal electroresistance and colossal magnetoresistance in spinel multiferroic CdCr2S4," *Appl. Phys. Lett.*, vol. 96, no. 12, p. 122109, Mar. 2010, doi: 10.1063/1.3368123.

[27] G. Kresse and J. Hafner, "Ab initio molecular dynamics for liquid metals," *Phys. Rev. B*, vol. 47, no. 1, pp. 558–561, Jan. 1993, doi: 10.1103/PhysRevB.47.558.

[28] G. Kresse and J. Furthmüller, "Efficiency of ab-initio total energy calculations for metals and semiconductors using a plane-wave basis set," *Comput. Mater. Sci.*, vol. 6, no. 1, pp. 15–50, Jul. 1996, doi: 10.1016/0927-0256(96)00008-0.

[29] P. Hohenberg and W. Kohn, "Inhomogeneous Electron Gas," *Phys. Rev.*, vol. 136, no. 3B, pp. B864–B871, Nov. 1964, doi: 10.1103/PhysRev.136.B864.

[30] J. P. Perdew, K. Burke, and M. Ernzerhof, "Generalized Gradient Approximation Made Simple [Phys. Rev. Lett. 77, 3865 (1996)]," *Phys. Rev. Lett.*, vol. 78, no. 7, pp. 1396–1396, Feb. 1997, doi: 10.1103/PhysRevLett.78.1396.

[31] P. E. Blöchl, "Projector augmented-wave method," *Phys. Rev. B*, vol. 50, no. 24, pp. 17953–17979, Dec. 1994, doi: 10.1103/PhysRevB.50.17953.

[32] H. J. Monkhorst and J. D. Pack, "Special points for Brillouin-zone integrations," *Phys. Rev. B*, vol. 13, no. 12, pp. 5188–5192, Jun. 1976, doi: 10.1103/PhysRevB.13.5188.

[33] Parrill and Lipkowitz, *Reviews in Computational Chemistry*. Wiley, 2016.

[34] S. A. Khandy, I. Islam, D. C. Gupta, R. Khenata, and A. Laref, "Lattice dynamics, mechanical stability and electronic structure of Fe-based Heusler semiconductors," *Sci. Rep.*, vol. 9, no. 1, p. 1475, Dec. 2019, doi: 10.1038/s41598-018-37740-y.

[35] P. Vinet, J. H. Rose, J. Ferrante, and J. R. Smith, "Universal features of the equation of state of solids," *J. Phys. Condens. Matter*, vol. 1, no. 11, pp. 1941–1963, Mar. 1989, doi: 10.1088/0953-8984/1/11/002.

[36] K. Sato, P. H. Dederichs, H. Katayama-Yoshida, and J. Kudrnovský, "Exchange interactions in diluted magnetic semiconductors," *J. Phys. Condens. Matter*, vol. 16, no. 48, pp. S5491–S5497, Dec. 2004, doi: 10.1088/0953-8984/16/48/003.

[37] M. Rostami, M. Afshari, and M. Moradi, "Bulk and surface half-metallicity of CsS in CsCl structure: A density functional theory study," *J. Alloys Compd.*, vol. 575, pp. 301–308, Oct. 2013, doi: 10.1016/j.jallcom.2013.05.171.

[38] A. Erkisi and G. Surucu, "The investigation of electronic, magnetic, mechanical, and lattice dynamical properties of Pd MX (M = Cr, Fe and X = Si and Ge) ferromagnetic half-Heusler metallics: an ab initio study," *Mater. Res. Express*, vol. 4, no. 6, p. 066504, Jun. 2017, doi: 10.1088/2053-1591/aa730e.

[39] A. Erkişi. "Magnetic orders and electronic behaviours of new chalcogenides Cu 3 MnCh 4 (Ch = S, Se and Te): An ab initio study." Philos. Mag., vol. 99, no. 15, pp. 1941–1955, Aug. 2019, doi: 10.1080/14786435.2019.1605221.

[40] A. Erkisi and G. Surucu, "The electronic and elasticity properties of new half-metallic chalcogenides," Philos. Mag., vol. 99, no. 4, pp. 513–529, Feb. 2019, doi: 10.1080/14786435.2018.1546960.

[41] N. V. Smith, "Photoelectron Energy Spectra and the Band Structures of the Noble Metals," *Phys. Rev. B*, vol. 3, no. 6, pp. 1862–1878, Mar. 1971, doi: 10.1103/PhysRevB.3.1862.

[42] C. Ambrosch-Draxl and J. O. Sofo, "Linear optical properties of solids within the full-potential linearized augmented planewave method," *Comput. Phys. Commun.*, vol. 175, no. 1, pp. 1–14, Jul. 2006, doi: 10.1016/j.cpc.2006.03.005.

[43] G. Surucu, K. Colakoglu, E. Deligoz, N. Korozlu, and Y. O. Ciftci, "The electronic and optical properties of mixed alloys," *Solid State Commun.*, vol. 150, no. 29–30, pp. 1413–1418, Aug. 2010, doi: 10.1016/j.ssc.2010.04.026.

[44] F. M, *Optical Properties of Solids, Oxford University Press, New York, NY.* 2001.

[45] M. Gajdoš, K. Hummer, G. Kresse, J. Furthmüller, and F. Bechstedt, "Linear optical properties in the projector-augmented wave methodology," *Phys. Rev. B*, vol. 73, no. 4, p. 045112, Jan. 2006, doi: 10.1103/PhysRevB.73.045112.

[46] M. Bokdam *et al.*, "Role of Polar Phonons in the Photo Excited State of Metal Halide Perovskites," *Sci. Rep.*, vol. 6, no. 1, p. 28618, Sep. 2016, doi: 10.1038/srep28618.

[47] A. Erkisi *et al.*, "First-principles investigation of LaGaO 3 and LaInO 3 lanthanum perovskite oxides" Philos. Mag., vol. 96, no. 19, pp. 2040–2058, Jul. 2016, doi: 10.1080/14786435.2016.1189100.

[48] A. Fahrenbruch and R. Bube, *Fundamentals of Solar Cells: Photovoltaic Solar Energy Conversion, Academic Press, New York.* 2012.

[49] S. Azam and A. H. Reshak, "Electronic Structure of 1,3-dicarbomethoxy4,6-benzenedicarboxylic acid: Density functional approach," *Int. J. Electrochem. Sci.*, vol. 8, no. 8, pp. 10359–10375, 2013.